gases

MDPI

Article

Testing the Experimental Unit at PT Lab for Collecting Data of CO_2 Solubility in Solvents

Stefania Moioli

GASP—Group on Advanced Separation Processes & GAS Processing, Dipartimento di Chimica, Materiali e Ingegneria Chimica "Giulio Natta", Politecnico di Milano, Piazza Leonardo da Vinci 32, 20133 Milan, Italy; stefania.moioli@polimi.it

Abstract

Carbon Capture, Utilization and Storage (CCUS) is a critical area of research due to its potential to significantly reduce CO_2 emissions from industrial processes and fossil fuel-based power generation. Aqueous amine solutions are commonly used as chemical solvents for CO_2 capture. However, their application is disfavoured by the high energy requirements and related operational costs, toxicity, and corrosion issues. To address these limitations, research is in general focused on developing novel solvents that can overcome the drawbacks of traditional amines. This development needs the study of phase equilibria in systems for which detailed physicochemical data are often scarce in the literature. In particular, understanding the solubility of gases (CO_2) in possible solvent mixtures is essential for evaluating their suitability for chemical or physical absorption processes. In this work, a dedicated setup was installed to generate the experimental data for these novel systems. This unit was designed to measure the solubility and diffusivity of gases in low-volatility liquids that could be alternative CO_2 solvents. A detailed experimental procedure was established, and the unit was initially validated by measuring CO_2 solubility in a 30 wt% monoethanolamine (MEA) solution, one of the most widely used industrial solvents. The experiments were conducted under conditions representing both the absorption and the regeneration sections of a CO_2 removal plant. The resulting equilibrium data were analyzed by employing several thermodynamic models, and the model providing the best representation was selected.

Keywords: CO_2 solubility; MEA; chemical absorption; PT lab

Academic Editor: Paola Ammendola

Received: 12 November 2025
Revised: 12 December 2025
Accepted: 16 December 2025
Published: 23 December 2025

1. Introduction

1.1. Carbon Capture, Utlization and Storage

The latest European report on the state of the climate [1] clearly illustrates the impact of climate change on Europe and the Arctic. In 2024, Europe was the continent experiencing the fastest warming, with a clear climate divide: eastern regions experienced extreme heat and drought, and western regions experienced extremely hot and humid weather. At the same time, Europe experienced the largest floods since 2013. The report also noted some positive developments: European cities are becoming more resilient to climate change, and, in 2024, a record 45% of electricity was generated from renewable sources. Dangerous climate change is taken into account in many literature sources, as for instance [2,3], that makes reference to the International Conference on Regional Climate, ICRC-CORDEX, which occurred in 2023 when about 500 scientists, stakeholders, and users came together in person and online to discuss the latest scientific advancements in regional climate

downscaling and in climate information for impacts and adaptation applications at regional and local levels.The report, produced by the EU's Copernicus Climate Change Service and the World Meteorological Organization, presented comprehensive data on the previous year's climate conditions in Europe and the Arctic. Some of the key findings are:

- In the European region and the Mediterranean Sea, annual sea surface temperatures were the highest on record;
- Glaciers in Scandinavia and Svalbard experienced the highest annual rates of mass loss;
- Western Europe experienced one of the ten wettest years on record;
- Southeastern Europe experienced below-average precipitation and the driest summer in a 12-year drought index;
- Europe experienced a record number of days of extreme heat and tropical nights and the area with subfreezing temperatures decreased.

Extreme weather events pose growing risks to Europe's urban areas. Therefore, urgent action is needed to increase their resilience. This action is essential to counter the projected increase in damage to cities caused by extreme weather, which could be up to ten times worse by 2100. Reducing the impact of climate change in Europe is an EU priority for the next five years.

Carbon Capture, Utilization and Storage (CCUS) is being explored as a strategy to reduce extreme weather events due to CO_2 emissions and is being considered in several sectors, including industrial manufacturing [4], power generation [5] also with WtE plants [6], and transportation [7]. To remove CO_2, for instance, adsorption-based technologies are under study, as reported in [8–10].

Among the available methods, CO_2 absorption using aqueous amine solutions is considered effective. Conventional amine-based solvents, such as monoethanolamine (MEA), diethanolamine (DEA), and methyldiethanolamine (MDEA), have long been employed in post-combustion CO_2 capture and other industrial CO_2 removal processes [11] due to their well-established reactivity with CO_2 and relatively rapid absorption kinetics. However, despite their widespread use and commercial maturity, these solvents present a number of inherent limitations that hinder their long-term sustainability and economic viability in large-scale applications. One of the primary concerns associated with conventional amines is the high energy demand required for solvent regeneration. The desorption process typically involves significant thermal input to reverse the chemical bonding between CO_2 and the amine, contributing to increased operational costs and reducing the overall efficiency of the carbon capture process. This high energy penalty is especially critical in industrial settings, where energy consumption directly impacts both economic feasibility and environmental performance. In addition to energy intensity, the use of traditional amines can lead to elevated operating costs stemming from solvent degradation and the need for frequent replacement. Thermal and oxidative degradation of amines [12,13], particularly under cyclic operation and high temperatures [14], leads to the formation of heat-stable salts and other degradation products that reduce absorption efficiency and also necessitate additional treatment steps, according to Rieder et al. [15]. Toxicity and environmental concerns also pose significant challenges according to Khakharia et al. [16]. Many amines and their degradation by-products can be harmful to human health and the environment if not properly managed [17,18]. Furthermore, the handling and disposal of these substances require strict regulatory compliance, adding complexity and cost to the process, considering that it may be lower than the lower limit of measurement for instruments [12,19]. Corrosiveness is another critical issue. Amine solutions, particularly when combined with acidic gases like CO_2, can become highly corrosive to carbon steel and other commonly used materials in gas absorption units. This necessitates the use of

corrosion inhibitors or more expensive corrosion-resistant alloys, further contributing to capital and maintenance expenditures.

Due to these limitations, there is growing interest in the development and characterization of alternative solvent systems, such as sterically hindered amines [20,21], amino acid salts [22], ionic liquids [23], deep eutectic solvents [24,25], and phase-change solvents [26,27] that aim to overcome the drawbacks of conventional amines [28] and maintain or improve CO_2 capture performance so as to enable the expansion of cost-efficient and environmentally sustainable CO_2 capture facilities. These next-generation solvents are designed to meet critical performance criteria, including rapid absorption rates, high CO_2 loading capacity, low regeneration energy requirements, minimal degradation and corrosiveness, reduced environmental impact, and lower overall cost [29].

To evaluate the suitability of new solvent candidates—especially those lacking comprehensive characterization in the literature—it is essential to analyze phase equilibria, particularly CO_2 solubility. Phase equilibria are also needed for the thermodynamic modeling of the system employed for simulation of the process. In the case of amine solvents, which are characterized by chemical absorption with the formation of ions in the liquid phase, the Electrolyte-NRTL model [30–33], with cubic EoS or PC-SAFT [34–39] for the description of the vapor phase, is employed. Another thermodynamic model that was developed for this type of system is the Extended-UNIQUAC [40–42]. Due to the scarcity of experimental data on emerging solvent systems, the Process Thermodynamics laboratory (PT lab) at Politecnico di Milano installed an experimental setup dedicated to measuring the solubility and diffusivity of gases in low-volatility liquids suitable for use as solvents.

This study focuses on defining a specific experimental procedure and validating the system by measuring the solubility of CO_2 in a 30 wt% Monoethanolamine (MEA) solution—one of the most widely used industrial solvents. The collected data are compared with existing literature values for the same mixture under identical operating conditions. Both absorption (at 40 °C) and regeneration (at 100 °C) conditions are considered in the analysis.

1.2. State of the Art

The solubility unit and experimental procedure were validated by comparing the collected data with literature values for a well-known solvent system. For this purpose, the CO_2 + MEA + H_2O system was selected, as it is extensively documented in the literature across a wide range of solvent compositions and temperatures representative of both absorption and regeneration conditions. This system has been widely studied due to the long-standing use of aqueous MEA solutions for CO_2 removal, since the 1930s [43], and is still regarded as the benchmark solvent for the industrial application in this field.

Specifically, for a 30 wt% MEA solution, several researchers (Table 1) have reported experimental CO_2 partial pressure data at different temperatures: Jou et al. [44], Ma'mun et al. [45], Kadiwala et al. [46], Aronu et al. [47], Dugas and Rochelle [48], Xu and Rochelle [49], Arshad et al. [50,51], Idris et al. [52] and Wanderley et al. [53].

As a first step, all the literature sources were cross-checked to assess the consistency of experimental data obtained under similar conditions of temperature, CO_2 loading, and partial pressure, ensuring a reliable reference for validating the experimental setup.

2. Materials and Methods

2.1. Materials

2.1.1. The Experimental Unit

The Process Thermodynamics laboratory (PT lab) is an experimental facility at Politecnico di Milano, established as part of the "Ingegneria Chimica—Energia (ICE)" collabora-

tion. It is located at the Department of Chemistry, Materials, and Chemical Engineering "Giulio Natta" [54,55]. The PT lab operates under the broader Process Design and Process Thermodynamics laboratory (PD&PT lab), that is managed by the GASP research group. It is equipped with experimental setups for the measurement of phase equilibria, including Vapor–Liquid Equilibrium (VLE), Vapor–Liquid–Liquid Equilibrium (VLLE), and Liquid–Liquid Equilibrium (LLE),gas solubility and diffusivity in solvents andkey physical properties as density and viscosity, which are essential for the comprehensive system characterization [56].

Table 1. State of the art in experimental data on CO_2 solubility in 30% wt. MEA aqueous solution.

Source	Temperature [°C]
Jou et al. (1995) [44]	0, 25, 40, 60, 80, 100, 120, 150
Ma'mun et al. (2005) [45]	120
Kadiwala et al. (2010) [46]	40
Aronu et al. (2011) [47]	40, 60, 80
Dugas and Rochelle (2011) [48]	40, 60, 80, 100
Xu and Rochelle (2011) [49]	from 100 to 174
Arshad et al. (2014) [50,51]	40, 80, 120
Idris et al. (2015) [52]	40, 80, 120
Wanderley et al. (2020) [53]	40, 80, 120

The setup was designed to suit the specific objectives of the equipment installed at the PT lab [57]. It consists of two main sections, with the left section (shown in Figure 1) designed for collecting experimental data at pressures up to 50 bar and the right section tailored for studying systems that form two liquid phases, with an operating pressure of up to about 7 bar.

Each section includes two cylindrical vessels:

- *D*1, shared between both sections, is filled with the gas to be absorbed—specifically, CO_2. It is equipped with a temperature sensor (TE10) and a pressure sensor (PT20, rated for 0–60 barg). It is connected to the CO_2 feed line via valves V15 and V1, and to the N_2 line via valves V16 and V1. Both CO_2 and N_2 gas cylinders are stored in a separate dedicated room.
- *D*2 (for high-pressure measurements) and D3 (for biphasic systems) are filled with the solvent and serve as the vessels where phase equilibrium takes place. Vessel *D*2 is connected to *D*1 via valve V2. The liquid is introduced through an inlet tube connected by valve V4, which also enables gas-phase sampling. A separate outlet tube is connected to the bottom of *D*2 and leads outside via valve V5, allowing liquid discharge at the end of each test. The vessel is equipped with a magnetic stirrer to ensure homogeneous mixing of the solvent, a temperature sensor (TE11), and two pressure transducers, PT21 (rated 0–10 bara) and PT22 (rated 0–60 barg), both with a precision of 0.2% of their respective full-scale values. An additional pressure sensor (rated 0–1 atm) can be employed for measuring low pressure values with higher precision. All sensor data are recorded and stored digitally using a data logger.

To maintain a constant temperature, *D*2 is placed inside a steel container with a removable lid, where thermostatic oil circulates after valve V12 is opened. A safety "too-full" tank is included in the system to prevent flooding in case of blockage in the circulation tubing, allowing excess oil to be safely discharged.

A vacuum pump is installed to lower the system pressure before and after solvent loading, ensuring proper initial conditions for each experiment. Additionally, a nitrogen line is incorporated to improve the efficiency of the discharge process (avoiding unin-

tended CO_2 dissolution during venting) and to inert the system before the start of each new test [58].

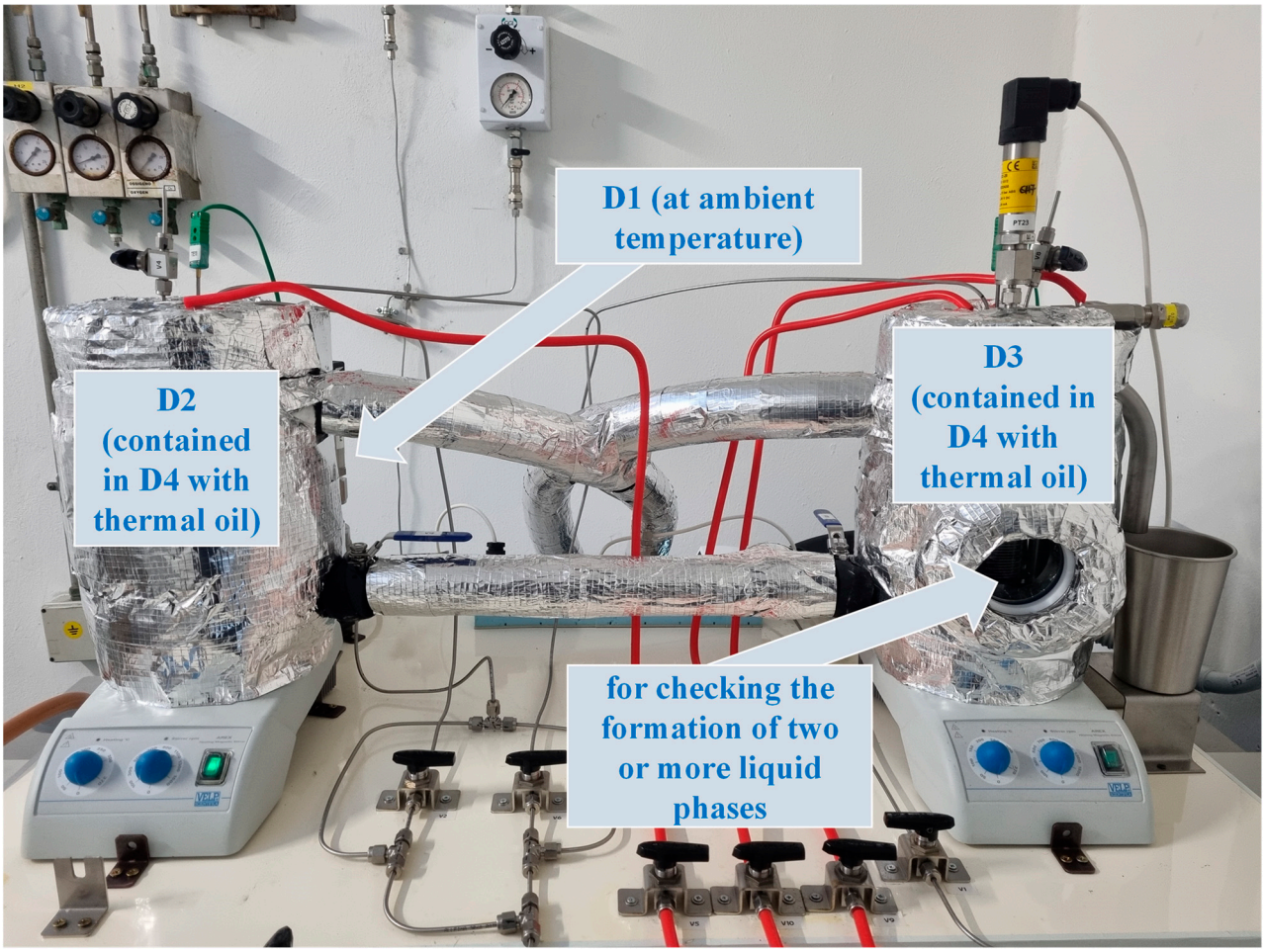

Figure 1. The unit for measuring solubility of gases into solvents at the PT lab of Politecnico di Milano.

An electronic balance with a maximum capacity of 520 g and a precision of 0.001 g is used for all weighing operations. Additionally, the PT lab is equipped with a dedicated section for preparing solvent mixtures under a nitrogen atmosphere, in order to prevent oxidative degradation of the amine components.

2.1.2. The Substances

A bottle of 40 L filled in with CO_2 with grade 4.5 from Sapio Srl, Monoethanolamine (CAS number 141-43-5) with 99% purity from Sigma Aldrich and demineralized water (ISO 3696 Q3, ASTM D 1193 TYPE 4) [59] were employed for the solubility tests. A bottle of nitrogen BIP from Sapio Srl was employed for discharging the liquid from the unit and in general for cleaning the unit from one test to the next before vacuum for emptying the vessels. After the first opening of the tank, the substances were stored in a nitrogen atmosphere.

2.2. Methods

2.2.1. Experimental Procedure

The procedure for the collection of the experimental points [57] is composed of several steps:

1. the system is flushed with nitrogen to make it inert;
2. the thermostatic bath is switched on;
3. when the temperature of the thermostatic fluid is equal to the temperature of the set point, the circulation of the thermostatic fluid is activated;
4. the vessel *D*1 is filled with CO_2 up to a defined pressure;
5. the vacuum pump is switched on until the pressure in vessel *D*2 is below 0.05 bar;
6. a known amount (mass) of the solvent, without CO_2, is added to vessel *D*2;
7. the vacuum pump is switched on again to remove the atmospheric air fed with the solvent, until the pressure in vessel *D*2 is below 0.05 bar;
8. part of the CO_2 contained in vessel *D*1 is transferred to vessel *D*2, up to a defined pressure in vessel *D*2;
9. the absorption time lasts until achieving the phase equilibrium, which is determined on the basis of the trend of the temperature and pressure sensors (even if the temperature of the experiment is set, in the case of absorption into a chemical solvent it varies when CO_2 is fed to vessel *D*2 and starts to be absorbed because of the exothermicity of the chemical reactions) after the values of temperature and pressure are stable for at least 4 h;
10. once equilibrium is achieved, the liquid phase is discharged together with the vapor phase (pressurization with N_2 is needed to empty the unit);
11. the liquid phase is weighed and may be analyzed.

The liquid phase is discharged in a predetermined amount of liquid to avoid the release of CO_2 because of modifications to the equilibrium conditions, in particular related to the transfer of liquid from equilibrium pressure to atmospheric pressure, in cases where the equilibrium pressure is high.

Each test is considered at equilibrium when the temperature and the pressure are stable for at least 4 h after stabilization of their profiles with time, so duration is much longer. No more than one test per day can be performed.

2.2.2. Theoretical Estimation of the Equilibrium Composition

The absorption of CO_2 was assessed through both theoretical calculations and validation with a material balance in the system. The theoretical equilibrium analysis follows the method outlined by Park and Sandall [60], which involves calculating the compressibility factor of the vapor phase using temperature and pressure data from the two vessels (*D*1 and *D*2), recorded before and after reaching equilibrium. These values are obtained from the solubility unit's temperature and pressure sensors.

The number of CO_2 moles transferred from vessel *D*1 to *D*2, along with the amount remaining in the vapor phase of *D*2 at equilibrium, are calculated. The difference between these values gives the quantity of CO_2 absorbed. Determining the moles of CO_2 in the vapor phase requires knowledge of both the tank volume and the solvent volume within the tank. The amount of solvent in the discharge tube before the discharge valve is not in contact with the vapor phase and is not considered for the determination of the equilibrium composition (this relevant point has not been found detailed in other papers in the literature, though it may cause a slight difference in the results).

In detail, the moles of gas in vessel *D*1 before the pressurization of vessel *D*2 are as in Equation (1) and the moles of gas in vessel *D*1 after the pressurization of vessel *D*2 are as in Equation (2).

$$n^{o}_{D1} = \frac{P_{D1,o} V_{D1}}{R\ T_{D1,o} Z_{D1.o}} \quad (1)$$

$$n_{D1}^{f} = \frac{P_{D1,f} V_{D1}}{R\, T_{D1,f} Z_{D1.f}} \quad (2)$$

The moles of gas fed to vessel $D2$ are then calculated as the difference (Equation (3)).

$$n_{D2}^{tot} = n_{D1}^{o} - n_{D1}^{f} \quad (3)$$

At equilibrium, the moles of gas remaining in vessel $D2$ are determined as in Equation (4)

$$n_{D2}^{f} = \frac{P_{D2,f}\, V_{D2}}{R\, T_{D2,f}\, Z_{D2.f}} \quad (4)$$

and the difference between the moles of gas fed to vessel $D2$ and this value provides the moles of absorbed CO_2 (Equation (5)).

$$n_{D2}^{sol} = n_{D2}^{tot} - n_{D2}^{f} \quad (5)$$

Then, the CO_2 loading, defined as the ratio of absorbed CO_2 moles and MEA moles in the solvent, is calculated based on the MEA quantity in the liquid phase at equilibrium.

Several Equations of State (EoSs) were evaluated for computing the compressibility factor Z of CO_2, including Van der Waals, Redlich–Kwong [61], Soave–Redlich–Kwong [62], and Peng–Robinson [63]. Additionally, Z was estimated using a spline interpolation function considered by Bientinesi et al. [64] based on experimental values from Perry and Green [65].

The expanded uncertainties were estimated with the methodology suggested by the NIST (National Institute of Standards and Technology) in 1992, which is based on the approach recommended by the CIPM (International Committee for Weights and Measures [66]).

In this study, the solvent losses in the vapor phase, caused by the vacuum pump operation and the system's operating temperature, were considered on the basis of experimental tests of charging, degassing and discharging the liquid solvent. The losses of solvent because of vacuum operation accounted for 0.74 g and the losses of solvent because of heating were equal to 0.22 g in the case of heating to 40 °C and to 0.765 g in the case of heating to 100 °C. These losses were considered in the evaluation of the amount of solvent at equilibrium and of P_{CO_2} at equilibrium.

The material balance was also checked by weighing the CO_2-free solvent charged into vessel $D2$ and the CO_2-rich solvent discharged after equilibrium, using a high-precision electronic balance.

3. Results

Results are reported in Table 2 and in Figure 2 for measurements at 40 °C and in Table 3 and in Figure 3 for measurements at 100 °C. Jou et al. [44] provided the loading values with two different analytical methods, gas chromatography and the $BaCO_3$-based method. In Figure 2 the experimental data by Jou et al. [44] refer to the analysis carried out with $BaCO_3$ and not to the one with GC considered previously [57]. Tables 4 and 5 report the comparison among the results obtained with the different thermodynamic methods considered in this work for temperature values equal to 40 °C and to 100 °C.

Table 2. Values of CO_2 partial pressure for different CO_2 loadings (α) for a mixture of MEA (30% wt.) and water at 40 °C experimentally obtained at the PT lab of Politecnico di Milano.

α [mol CO_2/mol MEA]	CO_2 Partial Pressure [kPa]
0.2032	2
0.3453	4
0.3710	4
0.3741	4
0.3830	4
0.4211	5
0.4406	5
0.4601	5
0.4994	7
0.6147	82
0.6222	87
0.6372	101
0.6383	113
0.6502	151
0.6941	304
0.7121	332
0.7206	362
0.7460	641
0.7608	624
0.7700	831
0.7725	748
0.7756	766
0.8033	953
0.8057	1163
0.8450	1434
0.8596	2037
0.8778	2060

Table 3. Values of CO_2 partial pressure for different CO_2 loadings (α) for a mixture of MEA (30% wt.) and water at 100 °C experimentally obtained at the PT lab of Politecnico di Milano.

α [mol CO_2/mol MEA]	CO_2 Partial Pressure [kPa]
0.1699	6
0.1797	6
0.1926	6
0.2124	6
0.2235	7
0.2251	7
0.2986	19
0.3485	31
0.3539	25
0.4967	270
0.5052	643
0.5549	607
0.5883	1638
0.6029	1188
0.6173	2041
0.6219	2298

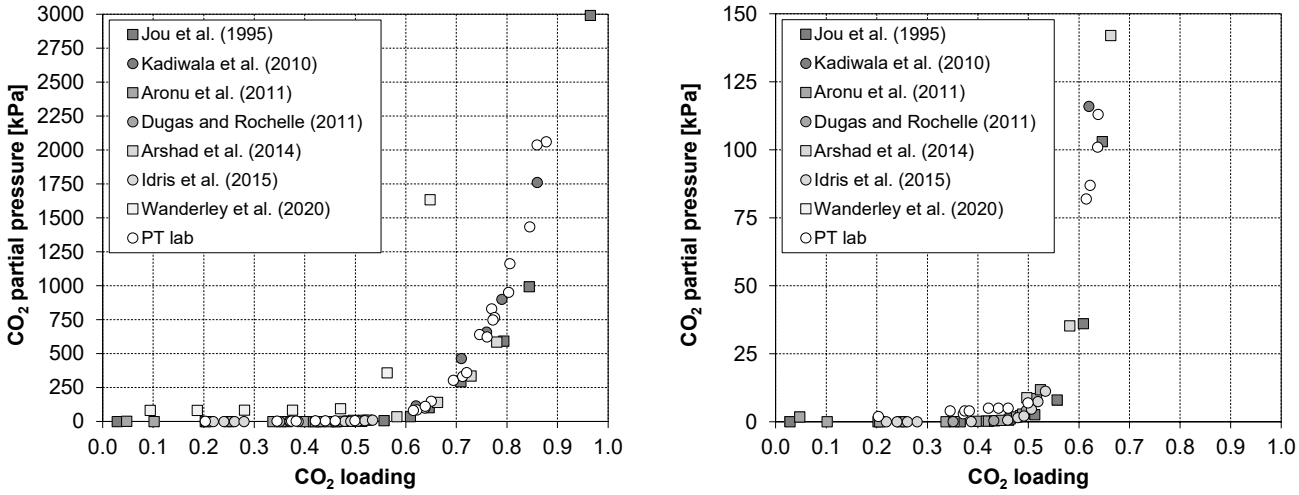

Figure 2. Comparison of the CO_2 partial pressure for different CO_2 loadings for a mixture of MEA (30% wt.) and water at 40 °C experimentally obtained at the PT lab of Politecnico di Milano with values from the literature (**a**) considering all points and (**b**) considering the detail for CO_2 partial pressures below 150 kPa.

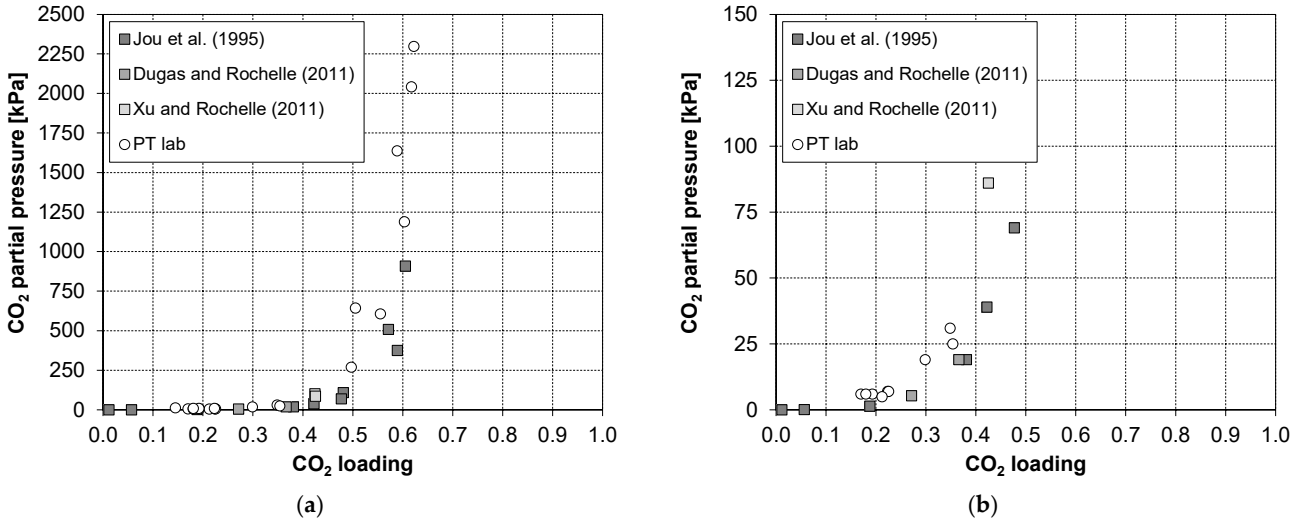

Figure 3. Comparison of the CO_2 partial pressure for different CO_2 loadings for a mixture of MEA (30% wt.) and water at 100 °C experimentally obtained at the PT lab of Politecnico di Milano with values from the literature (**a**) considering all points and (**b**) considering the detail for CO_2 partial pressures below 150 kPa.

Table 4. Values of different CO_2 loadings (α) for a mixture of MEA (30% wt.) and water at 40 °C obtained for CO_2 partial pressure considering the different methods described in Section 2.2.2.

Loading with PR EoS [molCO_2/molMEA]	Loading with VdW EoS [molCO_2/molMEA]	Loading with RK EoS [molCO_2/molMEA]	Loading with SRK EoS [molCO_2/molMEA]	Loading with Spline Interpolation [molCO_2/molMEA]
0.2032	0.2005	0.2020	0.2021	0.2024
0.3453	0.3372	0.3416	0.3419	0.3429
0.3710	0.3617	0.3667	0.3671	0.3684
0.3741	0.3648	0.3699	0.3703	0.3715
0.3830	0.3733	0.3786	0.3790	0.3803
0.4211	0.4097	0.4159	0.4163	0.4179
0.4406	0.4279	0.4348	0.4354	0.4372

Table 4. *Cont.*

Loading with PR EoS [molCO$_2$/molMEA]	Loading with VdW EoS [molCO$_2$/molMEA]	Loading with RK EoS [molCO$_2$/molMEA]	Loading with SRK EoS [molCO$_2$/molMEA]	Loading with Spline Interpolation [molCO$_2$/molMEA]
0.4601	0.4461	0.4537	0.4546	0.4566
0.4994	0.4827	0.4918	0.4929	0.4953
0.6147	0.5888	0.6028	0.6038	0.6075
0.6222	0.5947	0.6096	0.6109	0.6149
0.6372	0.6077	0.6237	0.6253	0.6295
0.6383	0.6094	0.6250	0.6262	0.6303
0.6502	0.6170	0.6351	0.6370	0.6414
0.6941	0.6522	0.6749	0.6764	0.6803
0.7121	0.6683	0.6920	0.6933	0.6969
0.7206	0.6721	0.6984	0.7007	0.7041
0.7460	0.6787	0.7151	0.7182	0.7160
0.7608	0.6949	0.7306	0.7329	0.7329
0.7700	0.6898	0.7334	0.7372	0.7322
0.7725	0.6974	0.7381	0.7414	0.7387
0.7756	0.6950	0.7389	0.7438	0.7398
0.8033	0.7090	0.7603	0.7653	0.7553
0.8057	0.6996	0.7571	0.7610	0.7441
0.8450	0.7058	0.7816	0.7893	0.7536
0.8596	0.6546	0.7664	0.7781	0.6771
0.8778	0.6359	0.7683	0.7927	0.6611

Table 5. Values of different CO_2 loadings (a) for a mixture of MEA (30% wt.) and water at 100 °C obtained for CO_2 partial pressure considering the different methods described in Section 2.2.2.

Loading with PR EoS [molCO$_2$/molMEA]	Average with VdW EoS [molCO$_2$/molMEA]	Average with RK EoS [molCO$_2$/molMEA]	Average with SRK EoS [molCO$_2$/molMEA]	Average with Spline Interpolation [molCO$_2$/molMEA]
0.1699	0.1671	0.1686	0.1687	0.1691
0.1797	0.1766	0.1783	0.1785	0.1789
0.1926	0.1894	0.1911	0.1912	0.1916
0.2124	0.2085	0.2106	0.2108	0.2112
0.2235	0.2188	0.2214	0.2217	0.2222
0.2251	0.2202	0.2229	0.2233	0.2238
0.2986	0.2892	0.2944	0.2954	0.2966
0.3485	0.3372	0.3434	0.3445	0.3461
0.3539	0.3440	0.3494	0.3498	0.3512
0.4967	0.4697	0.4845	0.4865	0.4902
0.5052	0.4585	0.4838	0.4873	0.4886
0.5549	0.5077	0.5335	0.5374	0.5397
0.5883	0.4683	0.5339	0.5456	0.5145
0.6029	0.5120	0.5620	0.5723	0.5611
0.6173	0.4762	0.5529	0.5619	0.5137
0.6219	0.4356	0.5373	0.5557	0.4653

4. Discussion

Figure 3 presents the experimental data obtained at the PT lab alongside reference data from various literature sources for a solvent system consisting of water and 30 wt% MEA at temperatures of 40 °C and 100 °C, for comparative purposes. Due to the inherent characteristics of the experimental apparatus—where pressure is not a controlled input but rather determined at equilibrium—it is not feasible to reproduce literature data points at identical values of CO_2 partial pressure and solvent loading. This limitation is typical of this class of experimental systems and is similarly reflected in the literature, where data

points from different studies are not aligned at identical values of CO_2 partial pressure or loading.

Therefore, the validity of the experimental procedure and apparatus is assessed based on the consistency of the observed trends with those reported in the literature [67], as demonstrated by prior studies such as those by Derks et al. [68], Ali and Aroua [69], and Dash et al. [70] for alternative amine systems. Consequently, it is not possible to define a precise percentage error between data sets from different sources; only an estimation with interpolation between two points of the same source and a comparison between the different sources could provide a value for the percentage error. For instance, for the experimental data collected at 40 °C, a value of % deviation from the experimental data by Jou et al. [44] for values of partial pressure of CO_2 higher than 10 kPa equal to 16.18% was obtained. This evaluation is to be considered approximate, because it is based on interpolation of data from the literature source and the ranges employed for interpolation are different for each data set because they depend on the experimental values reported in the literature source.

It can be extrapolated from Tables 4 and 5, which detail the loading obtained with the different thermodynamic methods considered in this work, that the differences among the methods are lower than 10%. In detail, Table 6 report the Absolute Average Deviation % (AAD%) calculated as the average of the absolute value of the difference between each loading obtained with the considered thermodynamic model and the one obtained with the PR EoS, divided by the loading obtained with the PR EoS. The results are reported in Table 6.

Table 6. Values of AAD% of the different methods described in Section 2.2.2.

Temperature [°C]	VdW EoS	RK EoS	SRK EoS	Spline Interpolation
40	7.63	3.48	3.06	4.10
100	8.23	3.74	3.03	4.62

The Peng–Robinson EoS was ultimately chosen as it most accurately represents the CO_2 gas phase and provides the best match for CO_2 partial pressure data. This selection is also confirmed in the literature [71,72].

The experimental results obtained at the PT lab are found to be in good agreement with the general trends reported in the literature at the considered temperatures. Although the data from Wanderley et al. [53] at 40 °C are included in Figure 3, they exhibit a noticeable deviation from the overall trend, which Wanderley et al. [53] attribute to pressure measurement issues encountered during their experiments.

5. Conclusions

Accurate measurement of CO_2 solubility in emerging solvents is crucial for assessing their potential in chemical and physical absorption applications. This study concentrated on the validation of the experimental setup located at the Process Thermodynamics lab (PT lab) of Politecnico di Milano, which has been specifically designed for acquiring solubility and diffusivity data of gases in liquids. Experimental measurements of CO_2 solubility in a 30 wt% MEA aqueous solution were performed and compared with data available in the literature. The consistency of the results confirms the reliability of the experimental system, establishing its suitability for future research on advanced solvent formulations.

Funding: This research received no external funding.

Data Availability Statement: The original contributions presented in this study are included in the article. Further inquiries can be directed to the corresponding author.

Conflicts of Interest: The author declares no conflict of interest.

Abbreviations

The following abbreviations are used in this manuscript:

CCUS	Carbon Capture, Utilization and Storage
MEA	MonoEthanolAmine

References

1. European Commission. Relazione Europea Sullo Stato del Clima: Il 2024 è Stato L'anno Più Caldo Mai Registrato in Europa. Available online: https://commission.europa.eu/news-and-media/news/2024-warmest-year-record-europe-finds-european-state-climate-report-2025-04-15_it (accessed on 16 January 2024).
2. Balmford, A.; Keshav, S.; Venmans, F.; Coomes, D.; Groom, B.; Madhavapeddy, A.; Swinfield, T. Realizing the social value of impermanent carbon credits. *Nat. Clim. Change* **2023**, *13*, 1172–1178. [CrossRef]
3. Lake, I.; Bukovsky, M.S. CORDEX—Advancing High-Resolution Climate Information and Its Use in Society. *BAMS* **2024**, *2024*, E1380–E1387. [CrossRef]
4. Baker, R.W.; Freeman, B.; Kniep, J.; Huang, Y.I.; Merkel, T.C. CO_2 Capture from Cement Plants and Steel Mills Using Membranes. *Ind. Eng. Chem. Res.* **2018**, *57*, 15963–15970. [CrossRef]
5. Moioli, S.; Ho, M.H.; Wiley, D.E.; Pellegrini, L.A. Thermodynamic Modeling of the System of CO_2 and Potassium Taurate Solution for Simulation of the Process of Carbon Dioxide Removal. *Chem. Eng. Res. Des.* **2018**, *136*, 834–845. [CrossRef]
6. Moioli, S.; Pellegrini, L.A.; Redolfi Riva, E.; Alberti, D.; Carrara, A. Application of Intercooling to the CO_2 Removal Section of an Italian Waste-To-Energy Plant. *Ind. Eng. Chem. Res.* **2025**, *64*, 9349–9372. [CrossRef]
7. Tavakoli, S.; Gamlem, G.M.; Kim, D.; Roussanaly, S.; Anantharaman, R.; Yum, K.K.; Valland, A. Exploring the technical feasibility of carbon capture onboard ships. *J. Clean. Prod.* **2024**, *452*, 142032. [CrossRef]
8. Ho, Q.D.; Rauls, E. Cavity Size Effects on the Adsorption of CO_2 on Pillar[n]arene Structures: A Density Functional Theory Study. *ChemistrySelect* **2023**, *8*, e202302266. [CrossRef]
9. Lin, W.; Cai, Z.; Lv, X.; Xiao, Q.; Chen, K.; Li, H.; Wang, C. Significantly Enhanced Carbon Dioxide Capture by Anion-Functionalized Liquid Pillar[5]arene through Multiple-Site Interactions. *Ind. Eng. Chem. Res.* **2019**, *58*, 16894–16900. [CrossRef]
10. Ho, Q.D.; Rauls, E. Ab initio study: Investigating the adsorption behaviors of polarized greenhouse gas molecules on pillar[5]arenes. *Mater. Today Commun.* **2023**, *36*, 106875. [CrossRef]
11. Pellegrini, L.A.; De Guido, G.; Moioli, S. Design of the CO_2 removal section for PSA tail gas treatment in hydrogen production plant. *Front. Energy Res.* **2020**, *8*, 77. [CrossRef]
12. Neerup, R.; Rasmussen, V.E.; Vinjarapu, S.H.B.; Larsen, A.H.; Shi, M.; Andersen, C.; Fuglsang, K.; Gram, L.K.; Nedenskov, J.; Kappel, J.; et al. Solvent degradation and emissions from a CO_2 capture pilot at a waste-to-energy plant. *J. Environ. Chem. Eng.* **2023**, *11*, 111411. [CrossRef]
13. Buvik, V.; Vevelstad, S.J.; Moser, P.; Wiechers, G.; Wanderley, R.R.; Monteiro, J.G.M.-S.; Knuutila, H.K. Degradation behaviour of fresh and pre-used ethanolamine. *Carbon Capture Sci. Technol.* **2023**, *7*, 100110. [CrossRef]
14. Feron, P.H.M.; Cousins, A.; Gao, S.; Liu, L.; Wang, J.; Wang, S.; Niu, H.; Yu, H.; Li, K.; Cottrell, A. Experimental performance assessment of a mono-ethanolamine-based post-combustion CO_2-capture at a coal-fired power station in China. *Greenh. Gases Sci. Technol.* **2017**, *7*, 486–499. [CrossRef]
15. Rieder, A.; Dhingra, S.; Khakharia, P.; Zangrilli, L.; Schallert, B.; Irons, R.; Unterberger, S.; van Os, P.; Goetheer, E. Understanding Solvent Degradation: A Study from Three Different Pilot Plants within the OCTAVIUS Project. *Energy Procedia* **2017**, *114*, 1195–1209. [CrossRef]
16. Khakharia, P.; Huizinga, A.; Jurado Lopez, C.; Sanchez Sanchez, C.; de Miguel Mercader, F.; Vlugt, T.J.H.; Goetheer, E. Acid Wash Scrubbing as a Countermeasure for Ammonia Emissions from a Postcombustion CO_2 Capture Plant. *Ind. Eng. Chem. Res.* **2014**, *53*, 13195–13204. [CrossRef]
17. Da Silva, E.F.; Kolderup, H.; Goetheer, E.; Hjarbo, K.W.; Huizinga, A.; Khakharia, P.; Tuinman, I.; Mejdell, T.; Zahlsen, K.; Vernstad, K.; et al. Emission studies from a CO_2 capture pilot plant. *Energy Procedia* **2013**, *37*, 778–783. [CrossRef]
18. Knudsen, J.N.; Bade, O.M.; Anheden, M.; Bjorklund, R.; Gorset, O.; Woodhouse, S. Novel Concept for Emission Control in Post Combustion Capture. *Energy Procedia* **2013**, *37*, 1804–1813. [CrossRef]
19. Fraboulet, I.; Chahen, L.; Lestremau, F.; Grimstvedt, A.; Schallert, B.; Moeller, B.C.; Järvinen, E. Round Robin Tests on Nitrosamines Analysis in the Effluents of a CO_2 Capture Pilot Plant. *Energy Procedia* **2016**, *86*, 252–261. [CrossRef]
20. Svensson, H.; Edfeldt, J.; Zejnullahu Velasco, V.; Hulteberg, C.; Karlsson, H.T. Solubility of carbon dioxide in mixtures of 2-amino-2-methyl-1-propanol and organic solvents. *Int. J. Greenh. Gas Control* **2014**, *27*, 247–254. [CrossRef]

21. Svensson, H.; Hulteberg, C.; Karlsson, H.T. Precipitation of AMP Carbamate in CO_2 Absorption Process. *Energy Procedia* **2014**, *63*, 750–757. [CrossRef]
22. Moioli, S.; Spatolisano, E.; Pellegrini, L.A. Techno-Economic Assessment for the Best Flexible Operation of the CO_2 Removal Section by Potassium Taurate Solvent in a Coal-Fired Power Plant. *Energies* **2024**, *17*, 1736. [CrossRef]
23. Krupiczka, R.; Rotkegel, A.; Ziobrowski, Z. Comparative study of CO_2 absorption in packed column using imidazolium based ionic liquids and MEA solution. *Sep. Purif. Technol.* **2015**, *149*, 228–236. [CrossRef]
24. Cichowska-Kopczyńska, I.; Nowosielski, B.; Warmińska, D. Deep Eutectic Solvents: Properties and Applications in CO_2 Separation. *Molecules* **2023**, *28*, 5293. [CrossRef] [PubMed]
25. Ruan, J.; Chen, L.; Qi, Z. Deep eutectic solvents as a versatile platform toward CO_2 capture and utilization. *Green Chem.* **2023**, *25*, 8328–8348. [CrossRef]
26. Papadopoulos, A.I.; Tzirakis, F.; Tsivintzelis, I.; Seferlis, P. Phase-Change Solvents and Processes for Postcombustion CO_2 Capture: A Detailed Review. *Ind. Eng. Chem. Res.* **2019**, *58*, 5088–5111. [CrossRef]
27. Zhang, S.; Shen, Y.; Wang, L.; Chen, J.; Lu, Y. Phase change solvents for post-combustion CO_2 capture: Principle, advances, and challenges. *Appl. Energy* **2019**, *239*, 876–897. [CrossRef]
28. Duy Ho, Q.; Rauls, E. Investigations of Functional Groups Effect on CO_2 Adsorption on Pillar[5]arenes Using Density Functional Theory Calculations. *ChemistrySelect* **2024**, *9*, e202401490. [CrossRef]
29. Budzianowski, W.M. Single solvents, solvent blends, and advanced solvent systems in CO_2 capture by absorption: A review. *Int. J. Glob. Warm.* **2015**, *7*, 184–225. [CrossRef]
30. Chen, C.C.; Britt, H.I.; Boston, J.F.; Evans, L.B. Local composition model for excess Gibbs energy of electrolyte systems. Part I: Single solvent, single completely dissociated electrolyte systems. *AIChE J.* **1982**, *28*, 588–596. [CrossRef]
31. Chen, C.C.; Evans, L.B. A local composition model for the excess Gibbs energy of aqueous electrolyte systems. *AIChE J.* **1986**, *32*, 444–454. [CrossRef]
32. Mock, B.; Evans, L.B.; Chen, C.C. Thermodynamic Representation of Phase Equilibria of Mixed-Solvent Electrolyte Systems. *AIChE J.* **1986**, *32*, 1655–1664. [CrossRef]
33. Song, Y.; Chen, C.-C. Symmetric Electrolyte Nonrandom Two-Liquid Activity Coefficient Model. *Ind. Eng. Chem. Res.* **2009**, *48*, 7788–7797. [CrossRef]
34. Gross, J.; Sadowski, G. Perturbed-Chain SAFT: An Equation of State Based on a Perturbation Theory for Chain Molecules. *Ind. Eng. Chem. Res.* **2001**, *40*, 1244–1260. [CrossRef]
35. Gross, J.; Sadowski, G. Modeling Polymer Systems Using the Perturbed-Chain Statistical Associating Fluid Theory Equation of State. *Ind. Eng. Chem. Res.* **2002**, *41*, 1084–1093. [CrossRef]
36. Gross, J.; Sadowski, G. Application of the Perturbed-Chain SAFT Equation of State to Associating Systems. *Ind. Eng. Chem. Res.* **2002**, *41*, 5510–5515. [CrossRef]
37. Gross, J.; Spuhl, O.; Tumakaka, F.; Sadowski, G. Modeling Copolymer Systems Using the Perturbed-Chain SAFT Equation of State. *Ind. Eng. Chem. Res.* **2003**, *42*, 1266–1274. [CrossRef]
38. Becker, F.; Buback, M.; Latz, H.; Sadowski, G.; Tumakaka, F. Cloud-point curves of ethylene−(meth)acrylate copolymers in fluid ethene up to high pressures and temperatures—Experimental study and PC–SAFT modeling. *Fluid Phase Equilib.* **2004**, *215*, 263–282. [CrossRef]
39. Kleiner, M.; Tumakaka, F.; Sadowski, G.; Latz, H.; Buback, M. Phase equilibria in polydisperse and associating copolymer solutions: Poly(ethene-co-(meth)acrylic acid)–monomer mixtures. *Fluid Phase Equilib.* **2006**, *241*, 113–123. [CrossRef]
40. Thomsen, K. Modeling electrolyte solutions with the extended universal quasichemical (UNIQUAC) model. *Pure Appl. Chem.* **2005**, *77*, 531–542. [CrossRef]
41. Thomsen, K.; Rasmussen, P. Modeling of vapor–liquid–solid equilibrium in gas–aqueous electrolyte systems. *Chem. Eng. Sci.* **1999**, *54*, 1787–1802. [CrossRef]
42. Thomsen, K.; Rasmussen, P.; Gani, R. Correlation and prediction of thermal properties and phase behaviour for a class of aqueous electrolyte systems. *Chem. Eng. Sci.* **1996**, *51*, 3675–3683. [CrossRef]
43. Bottoms, R.R. Organic Bases for Gas Purification. *Inf. Eng. Chem.* **1931**, *23*, 501–504. [CrossRef]
44. Jou, F.Y.; Mather, A.E.; Otto, F.D. The Solubility of CO_2 in a 30-Mass-Percent Monoethanolamine Solution. *Can. J. Chem. Eng.* **1995**, *73*, 140–147. [CrossRef]
45. Ma'mun, S.; Nilsen, R.; Svendsen, H.F.; Juliussen, O. Solubility of carbon dioxide in 30 mass % monoethanolamine and 50 mass % methyldiethanolamine solutions. *J. Chem. Eng. Data* **2005**, *50*, 630–634. [CrossRef]
46. Kadiwala, S.; Rayer, A.V.; Henni, A. High pressure solubility of carbon dioxide (CO_2) in aqueous piperazine solutions. *Fluid Phase Equilib.* **2010**, *292*, 20–28. [CrossRef]
47. Aronu, U.E.; Gondal, S.; Hessen, E.T.; Haug-Warberg, T.; Hartono, A.; Hoff, K.A.; Svendsen, H.F. Solubility of CO_2 in 15, 30, 45 and 60 mass% MEA from 40 to 120 °C and model representation using the extended UNIQUAC framework. *Chem. Eng. Sci.* **2011**, *66*, 6393–6406. [CrossRef]

48. Dugas, R.E.; Rochelle, G.T. CO_2 Absorption Rate into Concentrated Aqueous Monoethanolamine and Piperazine. *J. Chem. Eng. Data* **2011**, *56*, 2187–2195. [CrossRef]
49. Xu, Q.; Rochelle, G. Total pressure and CO_2 solubility at high temperature in aqueous amines. *Energy Procedia* **2011**, *4*, 117–124. [CrossRef]
50. Arshad, M.W.; Fosbøl, P.L.; von Solms, N.; Svendsen, H.F.; Thomsen, K. Equilibrium Solubility of CO_2 in Alkanolamines. *Energy Procedia* **2014**, *51*, 217–223. [CrossRef]
51. Arshad, M.W.; Svendsen, H.F.; Fosbøl, P.L.; von Solms, N.; Thomsen, K. Equilibrium Total Pressure and CO_2 Solubility in Binary and Ternary Aqueous Solutions of 2-(Diethylamino)ethanol (DEEA) and 3-(Methylamino)propylamine (MAPA). *J. Chem. Eng. Data* **2014**, *59*, 764–774. [CrossRef]
52. Idris, Z.; Peresunko, N.; Jens, K.J.; Eimer, D.A. Equilibrium solubility of carbon dioxide in aqueous solutions of 3-amino-1-propanol, 4-amino-1-butanol and 5-amino-1-pentanol at low partial pressures. *Fluid Phase Equilib.* **2015**, *387*, 81–87. [CrossRef]
53. Wanderley, R.R.; Pinto, D.D.D.; Knuutila, H.K. Investigating opportunities for water-lean solvents in CO_2 capture: VLE and heat of absorption in water-lean solvents containing MEA. *Sep. Purif. Technol.* **2020**, *231*, 115883. [CrossRef]
54. Barbieri, C.; Schiattarella, V.; Moioli, S.; Pellegrini, L.A.; Filippini, G.; de Angelis, A.R.; Fiori, G. Measurement and Correlation of Vapor–Liquid Equilibrium of Mixtures of 1,2-Propanediol or 1,4-Butanediol + 1,8-Diazabicyclo(5.4.0)undec-7-ene at 30 kPa. *Clean Technol.* **2025**, *7*, 3. [CrossRef]
55. Schiattarella, V.; Barbieri, C.; Moioli, S.; Pellegrini, L.A.; Filippini, G.; de Angelis, A.R.; Fiori, G. Study of Mixtures of 1,3-Propanediol+DBU and DBU+Sulfolane for a New Sustainable Solvent for CO_2 Removal. *Sustainability* **2024**, *16*, 11143. [CrossRef]
56. Moioli, S.; Pellegrini, L.A. Describing physical properties of CO_2 unloaded and loaded MDEA+PZ solutions. *Chem. Eng. Res. Des.* **2018**, *138*, 116–124. [CrossRef]
57. Moioli, S.; Schiattarella, V. New experimental data of CO_2 solubility in an amine solvent. *Chem. Eng. Trans.* **2025**, *117*, 379–384.
58. Bolis, L. Experimental Characterization of New Solvents and Simulation for CO_2 Absorption Application in Cement Plants. Master's Thesis, Politecnico di Milano, Milano, Italy, 2024.
59. *ISO 3696 Q3*; ASTM D 1193 TYPE 4. ASTM: West Conshohocken, PA, USA, 2024. Available online: https://www.idrochimica.com/wp-content/uploads/2024/10/DEPURATA-2024.pdf (accessed on 11 December 2025).
60. Park, M.K.; Sandall, O.C. Solubility of Carbon Dioxide and Nitrous Oxide in 50 mass Methyldiethanolamine. *J. Chem. Eng. Data* **2001**, *46*, 166–168. [CrossRef]
61. Redlich, O.; Kwong, J.N.S. On the thermodynamics of solutions. V: An equation of state. Fugacities of gaseous solutions. *Chem. Rev.* **1949**, *44*, 233–244. [CrossRef]
62. Soave, G. Equilibrium constants from a modified Redlich-Kwong equation of state. *Chem. Eng. Sci.* **1972**, *27*, 1197–1203. [CrossRef]
63. Peng, D.-Y.; Robinson, D.B. A New Two-Constant Equation of State. *Ind. Eng. Chem. Fundam.* **1976**, *15*, 59–64. [CrossRef]
64. Bientinesi, M.; Nicolella, C.; Maccone, P.; Boccaletti, G. Solubility and diffusivity of carbon dioxide in perfluoropolyethers. *Chem. Eng. Res. Des.* **2016**, *105*, 16–23. [CrossRef]
65. Perry, R.H.; Green, D.W. *Perry's Chemical Engineers' Handbook*, 7th ed.; McGraw-Hill International Editions: Singapore, 1997.
66. Taylor, B.N.; Kuyatt, C.E. *Guidelines for Evaluating and Expressing the Uncertainty of NIST Measurement Results*; National Institute of Standards and Technology: Gaithersburg, MD, USA, 1994.
67. Barbieri, C.; Moioli, S. Solubility Data of CO_2 in the MDEA+PZ Solvent: A Review of Experimental Data, Setups, and Procedures. *J. Chem. Eng. Data* **2025**, *70*, 4861–4879. [CrossRef]
68. Derks, P.W.J.; Hogendoorn, J.A.; Versteeg, G.F. Experimental and theoretical study of the solubility of carbon dioxide in aqueous blends of piperazine and N-methyldiethanolamine. *J. Chem. Thermodyn.* **2010**, *42*, 151–163. [CrossRef]
69. Ali, B.S.; Aroua, M.K. Effect of Piperazine on CO_2 Loading in Aqueous Solutions of MDEA at Low Pressure. *Int. J. Thermophys.* **2004**, *25*, 1863–1870. [CrossRef]
70. Dash, S.K.; Samanta, A.; Samanta, A.N.; Bandyopadhyay, S.S. Vapour liquid equilibria of carbon dioxide in dilute and concentrated aqueous solutions of piperazine at low to high pressure. *Fluid Phase Equilib.* **2011**, *300*, 145–154. [CrossRef]
71. Bottcher, N.; Taron, J.; Kolditz, O.; Liedl, R.; Park, C.-H. Comparison of equations of state for carbon dioxide for numerical simulations. In *Proceedings of the Models—Repositories of Knowledge, Leipzig, Germany, 16 September 2011*; IAHS Publications: Abingdon, UK, 2012; Volume 355.
72. Hosseini Jenab, M.; Abedinzadegan Abdi, M.; Najibi, S.H.; Vahidi, M.; Matin, N.S. Solubility of Carbon Dioxide in Aqueous Mixtures of N-Methyldiethanolamine + Piperazine + Sulfolane. *J. Chem. Eng. Data* **2005**, *50*, 583–586. [CrossRef]